Angular Analysis of $D^0 \to \pi^+\pi^-\mu^+\mu^-$ and $D^0 \to K^+K^-\mu^+\mu^-$ Decays and Search for CP Violation

R. Aaij *et al.*[*]
(LHCb Collaboration)

(Received 5 November 2021; accepted 2 May 2022; published 3 June 2022)

The first full angular analysis and an updated measurement of the decay-rate CP asymmetry of the $D^0 \to \pi^+\pi^-\mu^+\mu^-$ and $D^0 \to K^+K^-\mu^+\mu^-$ decays are reported. The analysis uses proton-proton collision data collected with the LHCb detector at center-of-mass energies of 7, 8, and 13 TeV. The dataset corresponds to an integrated luminosity of 9 fb^{-1}. The full set of CP -averaged angular observables and their CP asymmetries are measured as a function of the dimuon invariant mass. The results are consistent with expectations from the standard model and with CP symmetry.

DOI: 10.1103/PhysRevLett.128.221801

Rare charm decays with two oppositely charged leptons ($\ell^+\ell^-$) in the final state may proceed via the quark flavor-changing neutral-current (FCNC) process $c \to u\ell^+\ell^-$ and, as such, be sensitive to contributions from physics beyond the standard model (SM). They represent a unique probe to beyond-SM couplings to up-type quarks, which is complementary to recent studies of beauty quark $b \to s\ell^+\ell^-$ transitions, where a coherent pattern of deviations from the SM is emerging (e.g., see Refs. [1–3]). The loop-induced SM processes are more suppressed in charm than in the b-quark system due to the Glashow-Iliopoulos-Maiani mechanism [4]. The *short-distance* contributions to the inclusive $D \to X\mu^+\mu^-$ branching fraction, where D denotes a neutral or charged D meson and X represents one or more hadrons, are predicted to be of $\mathcal{O}(10^{-9})$ [5]. Sensitivity to FCNC processes via the measurement of branching fractions is limited due to the dominance of tree-level amplitudes involving intermediate resonances that subsequently decay into $\ell^+\ell^-$. These so-called *long-distance* contributions increase the SM branching fractions up to $\mathcal{O}(10^{-6})$ [5–8]. Studies of angular distributions and charge-parity (CP) asymmetries in the vicinity of intermediate resonances offer a access to observables with negligible theoretical uncertainties. These observables are sensitive to beyond-SM physics through the interference between long- and short-distance amplitudes. The values of these observables are negligibly small in the SM, but can reach the percent level in scenarios beyond the SM [7–18].

The LHCb Collaboration has previously reported the first observation of $D^0 \to h^+h^-\mu^+\mu^-$ decays, where h is either a pion or a kaon [19]. Charge-conjugate decays are implied throughout, unless stated otherwise. The measured branching fractions are in agreement with SM predictions [7,8]. Selected angular and CP asymmetries were also measured, with results in agreement with the SM and with CP symmetry [20]. However, a complete angular analysis of a rare charm decay is yet to be performed.

This Letter presents the first measurement of the full set of CP-averaged angular observables and CP asymmetries in $D^0 \to h^+h^-\mu^+\mu^-$ decays, together with an updated measurement of the CP asymmetry of the total decay rate, defined as

$$A_{CP} \equiv \frac{\Gamma(D^0 \to h^+h^-\mu^+\mu^-) - \Gamma(\bar{D}^0 \to h^+h^-\mu^+\mu^-)}{\Gamma(D^0 \to h^+h^-\mu^+\mu^-) + \Gamma(\bar{D}^0 \to h^+h^-\mu^+\mu^-)}, \quad (1)$$

where Γ indicates the total decay rate. The measurement uses proton-proton $(p\,p)$ collision data corresponding to an integrated luminosity of 9 fb^{-1}, collected by the LHCb experiment at center-of-mass energies of 7 and 8 TeV (run 1) and of 13 TeV (run 2). The analysis is an extension of that reported in Ref. [20]. It uses approximately three times as many signal decays and results for previously measured observables are superseded.

Semileptonic $D^0 \to h^+h^-\mu^+\mu^-$ decays are described by five independent kinematic variables: the squared invariant masses of the dimuon and dihadron systems, $q^2 \equiv m^2(\mu^+\mu^-)$ and $p^2 \equiv m^2(h^+h^-)$, and three decay angles θ_μ, θ_h, ϕ, (see Fig. S1 in the Supplemental Material [21]). Here, θ_μ is the angle between the μ^+ direction and the direction opposite to that of the D^0 meson in the dimuon rest frame; θ_h is the angle between the h^+ direction and the direction opposite to that of the D^0 meson in the dihadron rest frame; and ϕ is the angle between the two planes

[*]Full author list given at the end of the article.

formed by the dimuon and the dihadron systems in the rest frame of the D^0 meson [8,20,21]. In contrast to Ref. [20], the same definition of the angles is kept for D^0 and $\bar{D}^0$ mesons. Following Ref. [8] and defining $\vec{\Omega} \equiv (\cos\theta_\mu, \cos\theta_h, \phi)$, the differential decay rate is expressed as the sum of nine angular coefficients I_{1-9} that depend on q^2, p^2, and $\cos\theta_h$, multiplied by the terms $c_1 = 1$, $c_2 = \cos 2\theta_\mu$, $c_3 = \sin^2\theta_\mu \cos 2\phi$, $c_4 = \sin 2\theta_\mu \cos\phi$, $c_5 = \sin\theta_\mu \cos\phi$, $c_6 = \cos\theta_\mu$, $c_7 = \sin\theta_\mu \sin\phi$, $c_8 = \sin 2\theta_\mu \sin\phi$, and $c_9 = \sin^2\theta_\mu \sin 2\phi$, as

$$\frac{d^5\Gamma}{dq^2 dp^2 d\vec{\Omega}} = \frac{1}{2\pi}\sum_{i=1}^{9} c_i I_i. \tag{2}$$

Piecewise integration ranges in ϕ and $\cos\theta_\mu$ can be defined such that the coefficients I_{2-9} are expressed as angular asymmetries. For example, the coefficient I_2 is obtained as

$$I_2 = \int_{-\pi}^{\pi} d\phi \left[\int_{-1}^{-0.5} d\cos\theta_\mu + \int_{0.5}^{1} d\cos\theta_\mu - \int_{-0.5}^{0.5} d\cos\theta_\mu\right] \times \frac{d^5\Gamma}{dq^2 dp^2 d\vec{\Omega}}. \tag{3}$$

Corresponding integration ranges to obtain I_{3-9} are reported in Refs. [8,21]. The coefficients $I_{2,3,4,7}$ are even under CP transformations, while $I_{5,6,8,9}$ are CP odd. Since the term c_1 has no dependence on the decay angles, I_1 provides only a normalization factor and is not considered in this Letter.

This analysis measures the normalized observables $\langle I_{2-9}\rangle$ defined as

$$\langle I_{2,3,6,9}\rangle = \frac{1}{\Gamma}\int_{q^2_{\rm min}}^{q^2_{\rm max}} dq^2 \int_{p^2_{\rm min}}^{p^2_{\rm max}} dp^2 \int_{-1}^{+1} d\cos\theta_h I_{2,3,6,9},$$
$$\langle I_{4,5,7,8}\rangle = \frac{1}{\Gamma}\int_{q^2_{\rm min}}^{q^2_{\rm max}} dq^2 \int_{p^2_{\rm min}}^{p^2_{\rm max}} dp^2 \times \left[\int_{0}^{+1} d\cos\theta_h - \int_{-1}^{0} d\cos\theta_h\right] I_{4,5,7,8}, \tag{4}$$

where Γ is the decay rate in the considered region of dimuon mass. The integration boundaries $q^2_{\rm min}$, $q^2_{\rm max}$, and $p^2_{\rm max}$ depend on the dimuon-mass region, where $p^2_{\rm min} = 4m_h^2$ and m_h denotes the hadron mass. The integration in $\cos\theta_h$ is defined to optimize the sensitivity to beyond-SM effects by integrating out contributions from the dominant P-wave resonances in the dihadron system, which further decay into h^+h^- [8]. Experimentally, the observables are determined by measuring the decay-rate asymmetries of the data split by angular *tags* defined according to the piecewise integration of the decay rate. As an example, from Eqs. (3) and (4), $\langle I_2\rangle$ is measured as

$$\langle I_2\rangle = \frac{1}{\Gamma}[\Gamma(|\cos\theta_\mu| > 0.5) - \Gamma(|\cos\theta_\mu| < 0.5)]. \tag{5}$$

The observables $\langle I_{\rm i}\rangle$, measured separately for D^0 and $\bar{D}^0$ mesons, are labeled as $\langle I_{\rm i}\rangle$ and $\langle \bar{I}_{\rm i}\rangle$, respectively. Their CP average $\langle S_{\rm i}\rangle$ and asymmetry $\langle A_{\rm i}\rangle$ are defined as $\langle S_{\rm i}\rangle = \frac{1}{2}[\langle I_{\rm i}\rangle + (-)\langle \bar{I}_{\rm i}\rangle]$ and $\langle A_{\rm i}\rangle = \frac{1}{2}[\langle I_{\rm i}\rangle - (+)\langle \bar{I}_{\rm i}\rangle]$ for the CP-even (CP-odd) coefficients $\langle I_{2,3,4,7}\rangle$ ($\langle I_{5,6,8,9}\rangle$). The previously measured forward-backward asymmetry $A_{\rm FB}$ and triple-product asymmetry $A_{2\phi}$ [20] are related to $\langle S_6\rangle$ and $\langle A_9\rangle$, respectively. If only SM amplitudes contribute to the decay processes, the observables $\langle S_{5,6,7}\rangle$ are predicted to vanish and constitute SM null tests together with the CP asymmetries $\langle A_{2-9}\rangle$, which are expected to be below the current experimental sensitivity [8]. No predictions are available for the observables $\langle S_{2,3,4,8,9}\rangle$.

The analysis is performed using D^0 mesons that originate from decays of D^{*+} mesons directly produced in the primary $p\,p$ collision. The charge of the pion in the decay chain $D^{*+} \to D^0\pi^+$ is used to infer the flavor of the D^0 meson at its production. All observables are measured integrated in the full $m(\mu^+\mu^-)$ range and in $m(\mu^+\mu^-)$ regions defined according to the presence of the known intermediate resonances [20]. For $D^0 \to \pi^+\pi^-\mu^+\mu^-$ decays the regions are (low mass) below 525 MeV/c^2, (η) 525–565 MeV/c^2, (ρ^0/ω low) 565–780 MeV/c^2, (ρ^0/ω high) 780–950 MeV/c^2, (ϕ low) 950–1020 MeV/c^2, (ϕ high) 1020–1100 MeV/c^2, and (high mass) above 1100 MeV/c^2. For $D^0 \to K^+K^-\mu^+\mu^-$ decays, three regions are considered: (low mass) below 525 MeV/c^2, (η) 525–565 MeV/c^2, and only one region that combines the low and high ρ^0/ω region due to limited signal yields. The asymmetries are determined only in $m(\mu^+\mu^-)$ regions where a significant signal yield was previously observed [19]. No measurement is performed in the η region of both channels and in the high-mass region of $D^0 \to \pi^+\pi^-\mu^+\mu^-$. The integrated measurement includes candidates from all $m(\mu^+\mu^-)$ intervals. For each $m(\mu^+\mu^-)$ region, the kinematically allowed $m(h^+h^-)$ range up to a maximum of 1200 MeV/c^2, is considered. To avoid potential experimenter bias on the measured quantities, the observables were shifted by an unknown value during the development of the analysis and examined only after the analysis procedure was finalized.

The LHCb detector is a single-arm forward spectrometer described in detail in Ref. [22]. It provides high-precision tracking and good particle identification over a large range in momentum [23]. Simulation [24–31] is used to optimize the selection and to estimate variations of the reconstruction and selection efficiency across the decay phase space. Corrections to account for mismodeling of the charged-particle multiplicity of the events and of the particle-identification performance are applied using control channels in the data [32,33].

Events are selected online by a trigger that consists of a hardware stage, based on information from the muon systems, followed by a software stage, based on charged tracks that are displaced from any primary pp-interaction vertex (PV). A subsequent software trigger exploits a full event reconstruction [34] to select $D^0 \to h^+h^-\mu^+\mu^-$ candidates. Online selection requirements that have changed over data-taking periods are equalized in the off-line selection, which follows closely that of Ref. [20].

Candidate D^0 mesons are constructed off-line by combining four charged tracks, each having momentum larger than 3000 MeV/c and the momentum component transverse to the beam direction $p_T > 300$ MeV/c, that form a good-quality secondary vertex (SV) significantly displaced from any PV in the event. Two oppositely charged particles are required to be identified as muons and two as either pions or kaons. The D^0 candidates are required to have invariant mass in the range $1820 < m(h^+h^-\mu^+\mu^-) < 1940$ MeV/c^2 and to be consistent with originating from the associated PV, defined as the PV with respect to which the D^0 candidate has the lowest impact-parameter significance. The D^0 momentum is required to be aligned with the vector connecting the PV and the SV. The mass of the dihadron system is required to be less than 1200 MeV/c^2. The D^0 candidates are combined with low-momentum charged pions having $p_T > 120$ MeV/c, denoted as soft pions in the following, to form D^{*+} candidates. The D^{*+} decay vertex is required to coincide with the position of the associated PV. The difference between the masses of the D^{*+} and D^0 candidates, Δm, must be within $|\Delta m - 145.4\ \text{MeV}/c^2| < 0.6\ \text{MeV}/c^2$, corresponding to approximately ± 2 standard deviations in Δm resolution around the known value [35].

To suppress the combinatorial background formed with randomly associated tracks that accidentally fulfil the selection requirements, a boosted decision tree (BDT) algorithm [36,37] with gradient boosting [38] is employed. Simulated decays and data candidates from the sideband region $m(h^+h^-\mu^+\mu^-) > 1890$ MeV/c^2 are used as signal and background proxies, respectively. To have an unbiased estimate of the BDT performance, a cross validation is performed. The training samples are randomly split into two halves and the BDT classifier is applied to the subsample that has not been used in the training. Separate classifiers are trained for $D^0 \to \pi^+\pi^-\mu^+\mu^-$ and $D^0 \to K^+K^-\mu^+\mu^-$ decays and for run 1 and run 2 data samples to account for differences in decay kinematics and data-taking conditions, respectively. The variables used in the training are momentum and p_T of the soft pion, the largest distance of closest approach of the D^0 decay-product trajectories, the angle between the D^0 momentum and the vector connecting the PV and the SV, the fit quality of the SV and its spatial separation from the PV. Purely hadronic decays of the form $D^0 \to h^+h^-\pi^+\pi^-$ with two pions wrongly identified as muons are further reduced by requirements on muon identification [33,39]. The optimal working points of the BDT output selection and muon-identification thresholds are determined simultaneously by maximizing the quantity $\mathcal{S}/\sqrt{\mathcal{S}+\mathcal{B}}$, where $\mathcal{S}$ and $\mathcal{B}$ are the signal and background yields, respectively, determined from the data in the signal region defined as $1840 < m(h^+h^-\mu^+\mu^-) < 1890$ MeV/c^2. In the approximately 0.5% of events where multiple $D^0 \to \pi^+\pi^-\mu^+\mu^-$ candidates are reconstructed after the full selection, only one is kept at random. No multiple-candidate events are found for $D^0 \to K^+K^-\mu^+\mu^-$ decays.

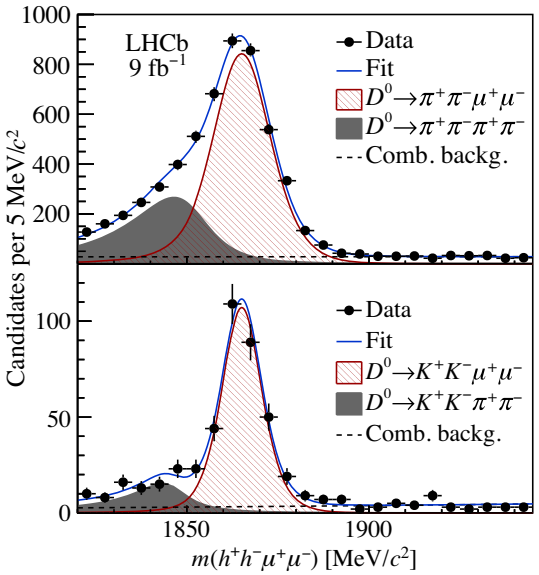

FIG. 1. Mass distribution of (top) $D^0 \to \pi^+\pi^-\mu^+\mu^-$ and (bottom) $D^0 \to K^+K^-\mu^+\mu^-$ candidates with fit projections overlaid.

The $m(h^+h^-\mu^+\mu^-)$ distributions for selected candidates are shown in Fig. 1. Unbinned maximum-likelihood fits to these distributions yield 3579 ± 71 $D^0 \to \pi^+\pi^-\mu^+\mu^-$ and 318 ± 19 $D^0 \to K^+K^-\mu^+\mu^-$ signal decays. The signal probability density function (PDF) is described by a Hypatia distribution [40] with parameters fixed from simulation, apart from two factors scaling the width and mean of the distribution to account for data-simulation differences. Misidentified hadronic decays are described by a Johnson S_U distribution [41] with parameters fixed from a fit to high-yield data samples of $D^0 \to h^+h^-\pi^+\pi^-$ decays with muon-mass hypothesis assigned to two pions and muon-identification criteria applied only to one of them. The combinatorial background is described by an exponential function with shape fixed from a fit to the candidates satisfying $|\Delta m - 145.4\ \text{MeV}/c^2| > 2\ \text{MeV}/c^2$, $\Delta m < 170$ MeV/c^2, and $1880 < m(h^+h^-\mu^+\mu^-) < 1945$ MeV/c^2.

The LHCb detector geometry, signal reconstruction, and selection requirements result in nonuniform efficiency across the five-dimensional phase space of the decays defined by p^2, q^2, θ_μ, θ_h, and ϕ. The efficiency variations

are corrected using a method developed in Refs. [20,42]. A BDT classifier with gradient boosting [36–38] is used to identify differences in the decay kinematics before and after reconstruction and selection. The BDT classifier is trained on simulation using the five-dimensional phase-space variables as input. From the classifier output, per-event candidate weights are derived that correspond to the inverse efficiency. To account for the different detector conditions, separate classifiers are trained for run 1 and run 2 data samples. As a consequence of the weighting, the effective statistical power of the $D^0 \to \pi^+\pi^-\mu^+\mu^-$ ($D^0 \to K^+K^-\mu^+\mu^-$) data sample is reduced by approximately 10% (6%).

To determine the CP asymmetry A_{CP}, the raw asymmetry in D^0- and $\bar{D}^0$-signal yields, $A_{CP}^{\rm raw}$, is corrected for $\mathcal{O}(1\%)$ nuisance asymmetries: differences in the production cross section of D^{*+} and D^{*-} mesons, A_P, and in the detection efficiencies of positively and negatively charged soft pions, A_D. The raw asymmetry for decays to the final state f is approximated as $A_{CP}^{\rm raw}(f) \approx A_{CP}(f) + A_P + A_D$. A high-yield control sample of $D^{*+} \to D^0(\to K^+K^-)\pi^+$ decays is used to determine the combined nuisance asymmetry as $A_P + A_D \approx A_{CP}^{\rm raw}(K^+K^-) - A_{CP}(K^+K^-)$, using $A_{CP}(K^+K^-) = (-0.06 \pm 0.18)\%$ from the independent measurement of Ref. [43]. In this procedure, the two-dimensional distribution of momentum and pseudorapidity of D^{*+} candidates in the control samples is equalized to that of the signal decays to account for differences in decay kinematics. Since the angular observables are measured independently for D^0 and $\bar{D}^0$ mesons, no correction for nuisance asymmetries is needed.

Each angular observable (or $A_{CP}^{\rm raw}$) is determined, independently in each dimuon-mass region, through simultaneous unbinned maximum-likelihood fits to the efficiency-corrected $m(h^+h^-\mu^+\mu^-)$ distributions of candidates split according to the angular tag (or D^0-meson flavor). The fits use the same model as described earlier, but with PDFs determined independently in each dimuon-mass region.

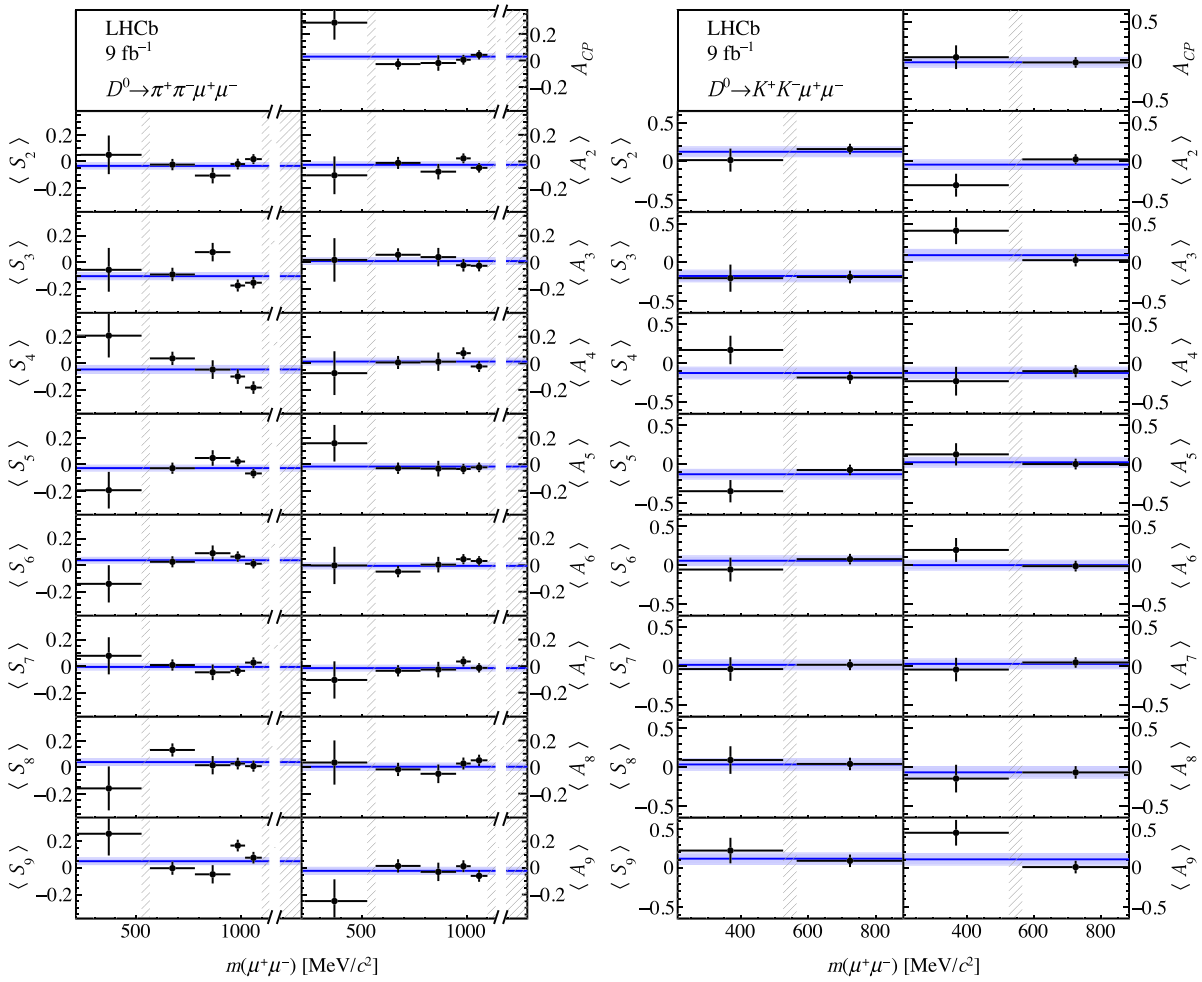

FIG. 2. Measured observables for (left) $D^0 \to \pi^+\pi^-\mu^+\mu^-$ and (right) $D^0 \to K^+K^-\mu^+\mu^-$ decays in $m(\mu^+\mu^-)$ regions. No measurement is performed in the regions indicated by the vertical gray bands. The horizontal bands correspond to the measurements integrated in the dimuon mass, including candidates from all $m(\mu^+\mu^-)$ ranges. The high-mass region of $D^0 \to \pi^+\pi^-\mu^+\mu^-$ extends to 1590.5 MeV/c^2 and has been truncated on the plots for a clearer visualization of the other regions.

The same PDFs are assumed when fitting the subsamples split by the tags, except for the measurement of $\langle I_2 \rangle$, where the mass shape of misidentified hadronic decays depends on the angular tag. The yield and angular observable (or A_{CP}^{raw}) of the three fit components (signal, misidentified, and combinatorial background) are the only floating parameters. The results for $\langle S_i \rangle$, $\langle A_i \rangle$, and A_{CP}, including both statistical and systematic uncertainties added in quadrature, are reported in Fig. 2. In general, the null-test observables show agreement with the SM predictions. A tabulated version is given in the Supplemental Material [21] together with the correlations between the observables, estimated using a bootstrapping technique [44].

Systematic uncertainties are typically between 10% and 50% of the statistical uncertainty, depending on the observable and the dimuon-mass region. These arise from the following sources: the model used in the mass fits; neglected background from partially reconstructed D_s^+ mesons, from D^{*+} candidates made of D^0 mesons combined with unrelated soft pions, and from D^{*+} candidates originating from decays of b-flavored hadrons; uncertainties in the estimation of the efficiency correction; the accuracy of the correction for nuisance charge asymmetries; the finite resolution of the angular variables. The leading systematic uncertainties are those related to the efficiency correction. These include residual biases on the observables due to efficiency variations that are not fully accounted for by the correction, the uncertainty coming from the limited size of the simulation sample, and effects due to potential residual differences between the data and simulation. The systematic uncertainties due to the efficiency correction are evaluated by repeating the analysis on either fully simulated decays or on simplified simulations that mimic the presence of data-simulation differences. The generation of the simplified simulations reproduces the $m(\mu^+\mu^-)$ and $m(h^+h^-)$ distributions observed in the data and is performed exploiting multithreaded architectures using the Hydra library [45,46].

The analysis procedure is validated using the more abundant $D^0 \to K^-\pi^+\mu^+\mu^-$ decay in the dimuon-mass range $675 < m(\mu^+\mu^-) < 875$ MeV/c^2, where the contribution from the $\rho^0/\omega \to \mu^+\mu^-$ decay is dominant. The decay is not sensitive to FCNC processes and is dominated by the SM tree-level amplitude. The analysis measures the angular observables serving as a SM null test ($\langle A_{2-9} \rangle$ and $\langle S_{5-7} \rangle$) to be consistent with zero within approximately 1%. As a further cross-check, the analysis is repeated on disjoint subsamples of the data selected according to criteria such as the magnetic-field orientation, which is reversed periodically during data taking; the number of PVs in the event; the transverse momentum of the D^{*+} and soft-pion candidates; and the minimum distance of the D^0 meson to the PV. The resulting variations of the measured observables are as expected according to statistical variations.

In summary, a measurement of the full set of CP-averaged angular observables and their CP asymmetries in $D^0 \to \pi^+\pi^-\mu^+\mu^-$ and $D^0 \to K^+K^-\mu^+\mu^-$ decays is reported, together with an updated measurement of A_{CP}. The analysis uses $p\,p$ collision data collected with the LHCb detector at center-of-mass energies of 7, 8, and 13 TeV, corresponding to an integrated luminosity of 9 fb^{-1}. This is the first full angular analysis of a rare charm decay ever performed. The measured null-test observables A_{CP}, $\langle S_{5-7} \rangle$, and $\langle A_{2-9} \rangle$ are in agreement with the SM null hypothesis with overall p values of 79% (0.8%) for $D^0 \to \pi^+\pi^-\mu^+\mu^-$ ($D^0 \to K^+K^-\mu^+\mu^-$) decays, corresponding to 0.3 (2.7) Gaussian standard deviations. These measurements will help constraining the parameters space of physics models extending the SM.

We express our gratitude to our colleagues in the CERN accelerator departments for the excellent performance of the LHC. We thank the technical and administrative staff at the LHCb institutes. We acknowledge support from CERN and from the national agencies: CAPES, CNPq, FAPERJ and FINEP (Brazil); MOST and NSFC (China); CNRS/IN2P3 (France); BMBF, DFG and MPG (Germany); INFN (Italy); NWO (Netherlands); MNiSW and NCN (Poland); MEN/IFA (Romania); MSHE (Russia); MICINN (Spain); SNSF and SER (Switzerland); NASU (Ukraine); STFC (United Kingdom); DOE NP and NSF (USA). We acknowledge the computing resources that are provided by CERN, IN2P3 (France), KIT and DESY (Germany), INFN (Italy), SURF (Netherlands), PIC (Spain), GridPP (United Kingdom), RRCKI and Yandex LLC (Russia), CSCS (Switzerland), IFIN-HH (Romania), CBPF (Brazil), PL-GRID (Poland) and NERSC (USA). We are indebted to the communities behind the multiple open-source software packages on which we depend. Individual groups or members have received support from ARC and ARDC (Australia); AvH Foundation (Germany); EPLANET, Marie Skłodowska-Curie Actions and ERC (European Union); A*MIDEX, ANR, IPhU and Labex P2IO, and Région Auvergne-Rhône-Alpes (France); Key Research Program of Frontier Sciences of CAS, CAS PIFI, CAS CCEPP, Fundamental Research Funds for the Central Universities, and Sci. & Tech. Program of Guangzhou (China); RFBR, RSF and Yandex LLC (Russia); GVA, XuntaGal and GENCAT (Spain); the Leverhulme Trust, the Royal Society and UKRI (United Kingdom).

[1] R. Aaij *et al.* (LHCb Collaboration), Branching Fraction Measurements of the Rare $B_s^0 \to \phi\mu^+\mu^-$ and $B_s^0 \to f_2'(1525)\mu^+\mu^-$ Decays, Phys. Rev. Lett. **127**, 151801 (2021).

[2] R. Aaij *et al.* (LHCb Collaboration), Test of lepton universality in beauty-quark decays, Nat. Phys. **18**, 277 (2022).

[3] R. Aaij *et al.* (LHCb Collaboration), Measurement of *CP* -Averaged Observables in the $B^0 \to K^{*0}\mu^+\mu^-$ Decay, Phys. Rev. Lett. **125**, 011802 (2020).

[4] S. L. Glashow, J. Iliopoulos, and L. Maiani, Weak interactions with lepton-hadron symmetry, Phys. Rev. D **2**, 1285 (1970).

[5] A. Paul, I. I. Bigi, and S. Recksiegel, On $D \to X_u\ell^+\ell^-$ within the Standard Model and frameworks like the littlest Higgs model with T parity, Phys. Rev. D **83**, 114006 (2011).

[6] S. Fajfer, N. Košnik, and S. Prelovšek, Updated constraints on new physics in rare charm decays, Phys. Rev. D **76**, 074010 (2007).

[7] L. Cappiello, O. Catà, and G. D'Ambrosio, Standard model prediction and new physics tests for $D^0 \to h_1^+h_2^-\ell^+\ell^-$ ($h = \pi, K$; $\ell = e, \mu$), J. High Energy Phys. 04 (2013) 135.

[8] S. De Boer and G. Hiller, Null tests from angular distributions in $D \to P_1P_2l^+l^-$, $l = e$, μ decays on and off peak, Phys. Rev. D **98**, 035041 (2018).

[9] S. Fajfer and S. Prelovšek, Effects of littlest Higgs model in rare D meson decays, Phys. Rev. D **73**, 054026 (2006).

[10] I. I. Bigi and A. Paul, On CP asymmetries in two-, three- and four-body D decays, J. High Energy Phys. 03 (2012) 021.

[11] A. Paul, A. de la Puente, and I. I. Bigi, Manifestations of warped extra dimension in rare charm decays and asymmetries, Phys. Rev. D **90**, 014035 (2014).

[12] S. Fajfer and N. Košnik, Resonance catalyzed CP asymmetries in $D \to P\ell^+\ell^-$, Phys. Rev. D **87**, 054026 (2013).

[13] S. Fajfer and N. Košnik, Prospects of discovering new physics in rare charm decays, Eur. Phys. J. C **75**, 567 (2015).

[14] S. de Boer and G. Hiller, Flavour and new physics opportunities with rare charm decays into leptons, Phys. Rev. D **93**, 074001 (2016).

[15] H. Gisbert, M. Golz, and D. S. Mitzel, Theoretical and experimental status of rare charm decays, Mod. Phys. Lett. A **36**, 2130002 (2021).

[16] R. Bause, M. Golz, G. Hiller, and A. Tayduganov, The new physics reach of null tests with $D \to \pi\ell\ell$ and $D_s \to K\ell\ell$ decays, Eur. Phys. J. C **80**, 65 (2020); **81**, 219(E) (2021).

[17] R. Bause, H. Gisbert, M. Golz, and G. Hiller, Exploiting *CP*-asymmetries in rare charm decays, Phys. Rev. D **101**, 115006 (2020).

[18] A. Bharucha, D. Boito, and C. Méaux, Disentangling QCD and new physics in $D^+ \to \pi^+\ell^+\ell^-$, J. High Energy Phys. 04 (2021) 158.

[19] R. Aaij *et al.* (LHCb Collaboration), Observation of D^0 Meson Decays to $\pi^+\pi^-\mu^+\mu^-$ and $K^+K^-\mu^+\mu^-$ Final States, Phys. Rev. Lett. **119**, 181805 (2017).

[20] R. Aaij *et al.* (LHCb Collaboration), Measurement of Angular and *CP* Asymmetries in $D^0 \to \pi^+\pi^-\mu^+\mu^-$ and $D^0 \to K^+K^-\mu^+\mu^-$ Decays, Phys. Rev. Lett. **121**, 091801 (2018).

[21] See Supplemental Material at http://link.aps.org/supplemental/10.1103/PhysRevLett.128.221801 for an explicit definition of the phase-space variables, all angular and *CP* -violating observables, their measured values and correlations in tabular form.

[22] A. A. Alves, Jr. *et al.* (LHCb Collaboration), The LHCb detector at the LHC, J. Instrum. **3**, S08005 (2008).

[23] R. Aaij *et al.* (LHCb Collaboration), LHCb detector performance, Int. J. Mod. Phys. A **30**, 1530022 (2015).

[24] T. Sjöstrand, S. Mrenna, and P. Skands, PYTHIA 6.4 physics and manual, J. High Energy Phys. 05 (2006) 026.

[25] T. Sjöstrand, S. Mrenna, and P. Skands, A brief introduction to PYTHIA 8.1, Comput. Phys. Commun. **178**, 852 (2008).

[26] I. Belyaev *et al.*, Handling of the generation of primary events in Gauss, the LHCb simulation framework, J. Phys. Conf. Ser. **331**, 032047 (2011).

[27] D. J. Lange, The EvtGen particle decay simulation package, Nucl. Instrum. Methods Phys. Res., Sect. A **462**, 152 (2001).

[28] N. Davidson, T. Przedzinski, and Z. Was, PHOTOS interface in C++: Technical and physics documentation, Comput. Phys. Commun. **199**, 86 (2016).

[29] J. Allison *et al.* (Geant4 Collaboration), Geant4 developments and applications, IEEE Trans. Nucl. Sci. **53**, 270 (2006).

[30] S. Agostinelli *et al.* (Geant4 Collaboration), Geant4: A simulation toolkit, Nucl. Instrum. Methods Phys. Res., Sect. A **506**, 250 (2003).

[31] M. Clemencic, G. Corti, S. Easo, C. R. Jones, S. Miglioranzi, M. Pappagallo, and P. Robbe, The LHCb simulation application, Gauss: Design, evolution and experience, J. Phys. Conf. Ser. **331**, 032023 (2011).

[32] L. Anderlini *et al.*, The PIDCalib package, Report No. LHCb-PUB-2016-021, 2016.

[33] R. Aaij *et al.*, Selection and processing of calibration samples to measure the particle identification performance of the LHCb experiment in Run 2, Eur. Phys. J. Tech. Instrum. **6**, 1 (2019).

[34] R. Aaij *et al.*, The LHCb trigger and its performance in 2011, J. Instrum. **8**, P04022 (2013).

[35] P. A. Zyla *et al.* (Particle Data Group), Review of particle physics, Prog. Theor. Exp. Phys. **2020**, 083C01 (2020).

[36] L. Breiman, J. H. Friedman, R. A. Olshen, and C. J. Stone, *Classification and Regression Trees* (Wadsworth International Group, Belmont, California, USA, 1984).

[37] B. P. Roe, H.-J. Yang, J. Zhu, Y. Liu, I. Stancu, and G. McGregor, Boosted decision trees as an alternative to artificial neural networks for particle identification, Nucl. Instrum. Methods Phys. Res., Sect. A **543**, 577 (2005).

[38] A. Hoecker *et al.*, TMVA - Toolkit for multivariate data analysis, Proc. Sci., ACAT2007 (**2007**) 040.

[39] F. Archilli *et al.*, Performance of the muon identification at LHCb, J. Instrum. **8**, P10020 (2013).

[40] D. Martínez Santos and F. Dupertuis, Mass distributions marginalized over per-event errors, Nucl. Instrum. Methods Phys. Res., Sect. A **764**, 150 (2014).

[41] N. L. Johnson, Systems of frequency curves generated by methods of translation, Biometrika **36**, 149 (1949).

[42] B. Viaud, On the potential of multivariate techniques for the determination of multidimensional efficiencies, Eur. Phys. J. Plus **131**, 191 (2016).

[43] R. Aaij *et al.* (LHCb Collaboration), Measurement of *CP* asymmetry in $D^0 \to K^-K^+$ and $D^0 \to \pi^-\pi^+$ decays, J. High Energy Phys. 07 (2014) 041.

[44] B. Efron, Bootstrap methods: Another look at the jackknife, Ann. Stat. **7**, 1 (1979).

[45] A. A. Alves, Jr., MultithreadCorner/Hydra, 10.5281/zenodo.1206261 (2018).

[46] A. A. Alves, Jr. and M. D. Sokoloff, Hydra: A C++ 11 framework for data analysis in massively parallel platforms, J. Phys. Conf. Ser. **1085**, 042013 (2018).

R. Aaij,[32] A. S. W. Abdelmotteleb,[56] C. Abellán Beteta,[50] F. Abudinén,[56] T. Ackernley,[60] B. Adeva,[46] M. Adinolfi,[54] H. Afsharnia,[9] C. Agapopoulou,[13] C. A. Aidala,[87] S. Aiola,[25] Z. Ajaltouni,[9] S. Akar,[65] J. Albrecht,[15] F. Alessio,[48] M. Alexander,[59] A. Alfonso Albero,[45] Z. Aliouche,[62] G. Alkhazov,[38] P. Alvarez Cartelle,[55] A. A. Alves Jr.,[65] S. Amato,[2] J. L. Amey,[54] Y. Amhis,[11] L. An,[48] L. Anderlini,[22] N. Andersson,[50] A. Andreianov,[38] M. Andreotti,[21] F. Archilli,[17] A. Artamonov,[44] M. Artuso,[68] K. Arzymatov,[42] E. Aslanides,[10] M. Atzeni,[50] B. Audurier,[12] S. Bachmann,[17] M. Bachmayer,[49] J. J. Back,[56] P. Baladron Rodriguez,[46] V. Balagura,[12] W. Baldini,[21] J. Baptista Leite,[1] M. Barbetti,[22,b] R. J. Barlow,[62] S. Barsuk,[11] W. Barter,[61] M. Bartolini,[55,c] F. Baryshnikov,[83] J. M. Basels,[14] S. Bashir,[34] G. Bassi,[29] B. Batsukh,[68] A. Battig,[15] A. Bay,[49] A. Beck,[56] M. Becker,[15] F. Bedeschi,[29] I. Bediaga,[1] A. Beiter,[68] V. Belavin,[42] S. Belin,[27] V. Bellee,[50] K. Belous,[44] I. Belov,[40] I. Belyaev,[41] G. Bencivenni,[23] E. Ben-Haim,[13] A. Berezhnoy,[40] R. Bernet,[50] D. Berninghoff,[17] H. C. Bernstein,[68] C. Bertella,[62] A. Bertolin,[28] C. Betancourt,[50] F. Betti,[48] Ia. Bezshyiko,[50] S. Bhasin,[54] J. Bhom,[35] L. Bian,[73] M. S. Bieker,[15] N. V. Biesuz,[21] S. Bifani,[53] P. Billoir,[13] A. Biolchini,[32] M. Birch,[61] F. C. R. Bishop,[55] A. Bitadze,[62] A. Bizzeti,[22,d] M. Bjørn,[63] M. P. Blago,[48] T. Blake,[56] F. Blanc,[49] S. Blusk,[68] D. Bobulska,[59] J. A. Boelhauve,[15] O. Boente Garcia,[46] T. Boettcher,[65] A. Boldyrev,[82] A. Bondar,[43] N. Bondar,[38,48] S. Borghi,[62] M. Borisyak,[42] M. Borsato,[17] J. T. Borsuk,[35] S. A. Bouchiba,[49] T. J. V. Bowcock,[60] A. Boyer,[48] C. Bozzi,[21] M. J. Bradley,[61] S. Braun,[66] A. Brea Rodriguez,[46] J. Brodzicka,[35] A. Brossa Gonzalo,[56] D. Brundu,[27] A. Buonaura,[50] L. Buonincontri,[28] A. T. Burke,[62] C. Burr,[48] A. Bursche,[72] A. Butkevich,[39] J. S. Butter,[32] J. Buytaert,[48] W. Byczynski,[48] S. Cadeddu,[27] H. Cai,[73] R. Calabrese,[21,e] L. Calefice,[15,13] S. Cali,[23] R. Calladine,[53] M. Calvi,[26,f] M. Calvo Gomez,[85] P. Camargo Magalhaes,[54] P. Campana,[23] A. F. Campoverde Quezada,[6] S. Capelli,[26,f] L. Capriotti,[20,g] A. Carbone,[20,g] G. Carboni,[31,h] R. Cardinale,[24,c] A. Cardini,[27] I. Carli,[4] P. Carniti,[26,f] L. Carus,[14] K. Carvalho Akiba,[32] A. Casais Vidal,[46] R. Caspary,[17] G. Casse,[60] M. Cattaneo,[48] G. Cavallero,[48] S. Celani,[49] J. Cerasoli,[10] D. Cervenkov,[63] A. J. Chadwick,[60] M. G. Chapman,[54] M. Charles,[13] Ph. Charpentier,[48] G. Chatzikonstantinidis,[53] C. A. Chavez Barajas,[60] M. Chefdeville,[8] C. Chen,[3] S. Chen,[4] A. Chernov,[35] V. Chobanova,[46] S. Cholak,[49] M. Chrzaszcz,[35] A. Chubykin,[38] V. Chulikov,[38] P. Ciambrone,[23] M. F. Cicala,[56] X. Cid Vidal,[46] G. Ciezarek,[48] P. E. L. Clarke,[58] M. Clemencic,[48] H. V. Cliff,[55] J. Closier,[48] J. L. Cobbledick,[62] V. Coco,[48] J. A. B. Coelho,[11] J. Cogan,[10] E. Cogneras,[9] L. Cojocariu,[37] P. Collins,[48] T. Colombo,[48] L. Congedo,[19,i] A. Contu,[27] N. Cooke,[53] G. Coombs,[59] I. Corredoira,[46] G. Corti,[48] C. M. Costa Sobral,[56] B. Couturier,[48] D. C. Craik,[64] J. Crkovská,[67] M. Cruz Torres,[1] R. Currie,[58] C. L. Da Silva,[67] S. Dadabaev,[83] L. Dai,[71] E. Dall'Occo,[15] J. Dalseno,[46] C. D'Ambrosio,[48] A. Danilina,[41] P. d'Argent,[48] A. Dashkina,[83] J. E. Davies,[62] A. Davis,[62] O. De Aguiar Francisco,[62] K. De Bruyn,[79] S. De Capua,[62] M. De Cian,[49] E. De Lucia,[23] J. M. De Miranda,[1] L. De Paula,[2] M. De Serio,[19,i] D. De Simone,[50] P. De Simone,[23] F. De Vellis,[15] J. A. de Vries,[80] C. T. Dean,[67] F. Debernardis,[19,i] D. Decamp,[8] V. Dedu,[10] L. Del Buono,[13] B. Delaney,[55] H.-P. Dembinski,[15] A. Dendek,[34] V. Denysenko,[50] D. Derkach,[82] O. Deschamps,[9] F. Desse,[11] F. Dettori,[27,j] B. Dey,[77] A. Di Canto,[48] A. Di Cicco,[23] P. Di Nezza,[23] S. Didenko,[83] L. Dieste Maronas,[46] H. Dijkstra,[48] V. Dobishuk,[52] C. Dong,[3] A. M. Donohoe,[18] F. Dordei,[27] A. C. dos Reis,[1] L. Douglas,[59] A. Dovbnya,[51] A. G. Downes,[8] M. W. Dudek,[35] L. Dufour,[48] V. Duk,[78] P. Durante,[48] J. M. Durham,[67] D. Dutta,[62] A. Dziurda,[35] A. Dzyuba,[38] S. Easo,[57] U. Egede,[69] V. Egorychev,[41] S. Eidelman,[43,a,k] S. Eisenhardt,[58] S. Ek-In,[49] L. Eklund,[86] S. Ely,[68] A. Ene,[37] E. Epple,[67] S. Escher,[14] J. Eschle,[50] S. Esen,[50] T. Evans,[48] L. N. Falcao,[1] Y. Fan,[6] B. Fang,[73] S. Farry,[60] D. Fazzini,[26,f] M. Féo,[48] A. Fernandez Prieto,[46] A. D. Fernez,[66] F. Ferrari,[20,g] L. Ferreira Lopes,[49] F. Ferreira Rodrigues,[2] S. Ferreres Sole,[32] M. Ferrillo,[50] M. Ferro-Luzzi,[48] S. Filippov,[39] R. A. Fini,[19] M. Fiorini,[21,e] M. Firlej,[34] K. M. Fischer,[63] D. S. Fitzgerald,[87] C. Fitzpatrick,[62] T. Fiutowski,[34] A. Fkiaras,[48] F. Fleuret,[12] M. Fontana,[13] F. Fontanelli,[24,c] R. Forty,[48] D. Foulds-Holt,[55] V. Franco Lima,[60] M. Franco Sevilla,[66] M. Frank,[48] E. Franzoso,[21] G. Frau,[17] C. Frei,[48] D. A. Friday,[59] J. Fu,[6] Q. Fuehring,[15] E. Gabriel,[32] G. Galati,[19,i] A. Gallas Torreira,[46] D. Galli,[20,g] S. Gambetta,[58,48] Y. Gan,[3] M. Gandelman,[2] P. Gandini,[25] Y. Gao,[5] M. Garau,[27] L. M. Garcia Martin,[56] P. Garcia Moreno,[45] J. García Pardiñas,[26,f] B. Garcia Plana,[46] F. A. Garcia Rosales,[12] L. Garrido,[45] C. Gaspar,[48] R. E. Geertsema,[32] D. Gerick,[17] L. L. Gerken,[15] E. Gersabeck,[62] M. Gersabeck,[62] T. Gershon,[56] D. Gerstel,[10] L. Giambastiani,[28] V. Gibson,[55] H. K. Giemza,[36] A. L. Gilman,[63] M. Giovannetti,[23,h] A. Gioventù,[46] P. Gironella Gironell,[45] C. Giugliano,[21,e] K. Gizdov,[58] E. L. Gkougkousis,[48] V. V. Gligorov,[13] C. Göbel,[70] E. Golobardes,[85] D. Golubkov,[41] A. Golutvin,[61,83] A. Gomes,[1,l] S. Gomez Fernandez,[45] F. Goncalves Abrantes,[63] M. Goncerz,[35] G. Gong,[3] P. Gorbounov,[41] I. V. Gorelov,[40] C. Gotti,[26] E. Govorkova,[48]

J. P. Grabowski,[17] T. Grammatico,[13] L. A. Granado Cardoso,[48] E. Graugés,[45] E. Graverini,[49] G. Graziani,[22] A. Grecu,[37] L. M. Greeven,[32] N. A. Grieser,[4] L. Grillo,[62] S. Gromov,[83] B. R. Gruberg Cazon,[63] C. Gu,[3] M. Guarise,[21] M. Guittiere,[11] P. A. Günther,[17] E. Gushchin,[39] A. Guth,[14] Y. Guz,[44] T. Gys,[48] T. Hadavizadeh,[69] G. Haefeli,[49] C. Haen,[48] J. Haimberger,[48] T. Halewood-leagas,[60] P. M. Hamilton,[66] J. P. Hammerich,[60] Q. Han,[7] X. Han,[17] T. H. Hancock,[63] E. B. Hansen,[62] S. Hansmann-Menzemer,[17] N. Harnew,[63] T. Harrison,[60] C. Hasse,[48] M. Hatch,[48] J. He,[6,m] M. Hecker,[61] K. Heijhoff,[32] K. Heinicke,[15] R. D. L. Henderson,[69,56] A. M. Hennequin,[48] K. Hennessy,[60] L. Henry,[48] J. Heuel,[14] A. Hicheur,[2] D. Hill,[49] M. Hilton,[62] S. E. Hollitt,[15] R. Hou,[7] Y. Hou,[8] J. Hu,[17] J. Hu,[72] W. Hu,[7] X. Hu,[3] W. Huang,[6] X. Huang,[73] W. Hulsbergen,[32] R. J. Hunter,[56] M. Hushchyn,[82] D. Hutchcroft,[60] D. Hynds,[32] P. Ibis,[15] M. Idzik,[34] D. Ilin,[38] P. Ilten,[65] A. Inglessi,[38] A. Ishteev,[83] K. Ivshin,[38] R. Jacobsson,[48] H. Jage,[14] S. Jakobsen,[48] E. Jans,[32] B. K. Jashal,[47] A. Jawahery,[66] V. Jevtic,[15] X. Jiang,[4] M. John,[63] D. Johnson,[64] C. R. Jones,[55] T. P. Jones,[56] B. Jost,[48] N. Jurik,[48] S. H. Kalavan Kadavath,[34] S. Kandybei,[51] Y. Kang,[3] M. Karacson,[48] M. Karpov,[82] J. W. Kautz,[65] F. Keizer,[48] D. M. Keller,[68] M. Kenzie,[56] T. Ketel,[33] B. Khanji,[15] A. Kharisova,[84] S. Kholodenko,[44] T. Kirn,[14] V. S. Kirsebom,[49] O. Kitouni,[64] S. Klaver,[32] N. Kleijne,[29] K. Klimaszewski,[36] M. R. Kmiec,[36] S. Koliiev,[52] A. Kondybayeva,[83] A. Konoplyannikov,[41] P. Kopciewicz,[34] R. Kopecna,[17] P. Koppenburg,[32] M. Korolev,[40] I. Kostiuk,[32,52] O. Kot,[52] S. Kotriakhova,[21,38] P. Kravchenko,[38] L. Kravchuk,[39] R. D. Krawczyk,[48] M. Kreps,[56] F. Kress,[61] S. Kretzschmar,[14] P. Krokovny,[43,k] W. Krupa,[34] W. Krzemien,[36] J. Kubat,[17] M. Kucharczyk,[35] V. Kudryavtsev,[43,k] H. S. Kuindersma,[32,33] G. J. Kunde,[67] T. Kvaratskheliya,[41] D. Lacarrere,[48] G. Lafferty,[62] A. Lai,[27] A. Lampis,[27] D. Lancierini,[50] J. J. Lane,[62] R. Lane,[54] G. Lanfranchi,[23] C. Langenbruch,[14] J. Langer,[15] O. Lantwin,[83] T. Latham,[56] F. Lazzari,[29,n] R. Le Gac,[10] S. H. Lee,[87] R. Lefèvre,[9] A. Leflat,[40] S. Legotin,[83] O. Leroy,[10] T. Lesiak,[35] B. Leverington,[17] H. Li,[72] P. Li,[17] S. Li,[7] Y. Li,[4] Y. Li,[4] Z. Li,[68] X. Liang,[68] T. Lin,[61] R. Lindner,[48] V. Lisovskyi,[15] R. Litvinov,[27] G. Liu,[72] H. Liu,[6] Q. Liu,[6] S. Liu,[4] A. Lobo Salvia,[45] A. Loi,[27] J. Lomba Castro,[46] I. Longstaff,[59] J. H. Lopes,[2] S. López Soliño,[46] G. H. Lovell,[55] Y. Lu,[4] C. Lucarelli,[22,b] D. Lucchesi,[28,o] S. Luchuk,[39] M. Lucio Martinez,[32] V. Lukashenko,[32,52] Y. Luo,[3] A. Lupato,[62] E. Luppi,[21,e] O. Lupton,[56] A. Lusiani,[29,p] X. Lyu,[6] L. Ma,[4] R. Ma,[6] S. Maccolini,[20,g] F. Machefert,[11] F. Maciuc,[37] V. Macko,[49] P. Mackowiak,[15] S. Maddrell-Mander,[54] O. Madejczyk,[34] L. R. Madhan Mohan,[54] O. Maev,[38] A. Maevskiy,[82] D. Maisuzenko,[38] M. W. Majewski,[34] J. J. Malczewski,[35] S. Malde,[63] B. Malecki,[48] A. Malinin,[81] T. Maltsev,[43,k] H. Malygina,[17] G. Manca,[27,j] G. Mancinelli,[10] D. Manuzzi,[20,g] D. Marangotto,[25,q] J. Maratas,[9,r] J. F. Marchand,[8] U. Marconi,[20] S. Mariani,[22,b] C. Marin Benito,[48] M. Marinangeli,[49] J. Marks,[17] A. M. Marshall,[54] P. J. Marshall,[60] G. Martelli,[78] G. Martellotti,[30] L. Martinazzoli,[48,f] M. Martinelli,[26,f] D. Martinez Santos,[46] F. Martinez Vidal,[47] A. Massafferri,[1] M. Materok,[14] R. Matev,[48] A. Mathad,[50] V. Matiunin,[41] C. Matteuzzi,[26] K. R. Mattioli,[87] A. Mauri,[32] E. Maurice,[12] J. Mauricio,[45] M. Mazurek,[48] M. McCann,[61] L. Mcconnell,[18] T. H. Mcgrath,[62] N. T. Mchugh,[59] A. McNab,[62] R. McNulty,[18] J. V. Mead,[60] B. Meadows,[65] G. Meier,[15] N. Meinert,[76] D. Melnychuk,[36] S. Meloni,[26,f] M. Merk,[32,80] A. Merli,[25,q] L. Meyer Garcia,[2] M. Mikhasenko,[75,s] D. A. Milanes,[74] E. Millard,[56] M. Milovanovic,[48] M.-N. Minard,[8] A. Minotti,[26,f] L. Minzoni,[21,e] S. E. Mitchell,[58] B. Mitreska,[62] D. S. Mitzel,[15] A. Mödden,[15] R. A. Mohammed,[63] R. D. Moise,[61] S. Mokhnenko,[82] T. Mombächer,[46] I. A. Monroy,[74] S. Monteil,[9] M. Morandin,[28] G. Morello,[23] M. J. Morello,[29,p] J. Moron,[34] A. B. Morris,[75] A. G. Morris,[56] R. Mountain,[68] H. Mu,[3] F. Muheim,[58,48] M. Mulder,[79] D. Müller,[48] K. Müller,[50] C. H. Murphy,[63] D. Murray,[62] R. Murta,[61] P. Muzzetto,[27] P. Naik,[54] T. Nakada,[49] R. Nandakumar,[57] T. Nanut,[48] I. Nasteva,[2] M. Needham,[58] N. Neri,[25,q] S. Neubert,[75] N. Neufeld,[48] R. Newcombe,[61] E. M. Niel,[11] S. Nieswand,[14] N. Nikitin,[40] N. S. Nolte,[64] C. Normand,[8] C. Nunez,[87] A. Oblakowska-Mucha,[34] V. Obraztsov,[44] T. Oeser,[14] D. P. O'Hanlon,[54] S. Okamura,[21] R. Oldeman,[27,j] F. Oliva,[58] M. E. Olivares,[68] C. J. G. Onderwater,[79] R. H. O'Neil,[58] J. M. Otalora Goicochea,[2] T. Ovsiannikova,[41] P. Owen,[50] A. Oyanguren,[47] K. O. Padeken,[75] B. Pagare,[56] P. R. Pais,[48] T. Pajero,[63] A. Palano,[19] M. Palutan,[23] Y. Pan,[62] G. Panshin,[84] A. Papanestis,[57] M. Pappagallo,[19,i] L. L. Pappalardo,[21,e] C. Pappenheimer,[65] W. Parker,[66] C. Parkes,[62] B. Passalacqua,[21] G. Passaleva,[22] A. Pastore,[19] M. Patel,[61] C. Patrignani,[20,g] C. J. Pawley,[80] A. Pearce,[48,57] A. Pellegrino,[32] M. Pepe Altarelli,[48] S. Perazzini,[20] D. Pereima,[41] A. Pereiro Castro,[46] P. Perret,[9] M. Petric,[59,48] K. Petridis,[54] A. Petrolini,[24,c] A. Petrov,[81] S. Petrucci,[58] M. Petruzzo,[25] T. T. H. Pham,[68] A. Philippov,[42] R. Piandani,[6] L. Pica,[29,p] M. Piccini,[78] B. Pietrzyk,[8] G. Pietrzyk,[49] M. Pili,[63] D. Pinci,[30] F. Pisani,[48] M. Pizzichemi,[26,48,f] Resmi P. K,[10] V. Placinta,[37] J. Plews,[53] M. Plo Casasus,[46] F. Polci,[13] M. Poli Lener,[23] M. Poliakova,[68] A. Poluektov,[10] N. Polukhina,[83,t] I. Polyakov,[68] E. Polycarpo,[2] S. Ponce,[48] D. Popov,[6,48] S. Popov,[42] S. Poslavskii,[44] K. Prasanth,[35] L. Promberger,[48] C. Prouve,[46] V. Pugatch,[52] V. Puill,[11] H. Pullen,[63] G. Punzi,[29,u] H. Qi,[3] W. Qian,[6] J. Qin,[6] N. Qin,[3] R. Quagliani,[49] B. Quintana,[8] N. V. Raab,[18] R. I. Rabadan Trejo,[6] B. Rachwal,[34] J. H. Rademacker,[54] M. Rama,[29] M. Ramos Pernas,[56] M. S. Rangel,[2] F. Ratnikov,[42,82] G. Raven,[33]

M. Reboud,[8] F. Redi,[49] F. Reiss,[62] C. Remon Alepuz,[47] Z. Ren,[3] V. Renaudin,[63] R. Ribatti,[29] S. Ricciardi,[57] K. Rinnert,[60] P. Robbe,[11] G. Robertson,[58] A. B. Rodrigues,[49] E. Rodrigues,[60] J. A. Rodriguez Lopez,[74] E. R. R. Rodriguez Rodriguez,[46] A. Rollings,[63] P. Roloff,[48] V. Romanovskiy,[44] M. Romero Lamas,[46] A. Romero Vidal,[46] J. D. Roth,[87] M. Rotondo,[23] M. S. Rudolph,[68] T. Ruf,[48] R. A. Ruiz Fernandez,[46] J. Ruiz Vidal,[47] A. Ryzhikov,[82] J. Ryzka,[34] J. J. Saborido Silva,[46] N. Sagidova,[38] N. Sahoo,[56] B. Saitta,[27,j] M. Salomoni,[48] C. Sanchez Gras,[32] R. Santacesaria,[30] C. Santamarina Rios,[46] M. Santimaria,[23] E. Santovetti,[31,h] D. Saranin,[83] G. Sarpis,[14] M. Sarpis,[75] A. Sarti,[30] C. Satriano,[30,v] A. Satta,[31] M. Saur,[15] D. Savrina,[41,40] H. Sazak,[9] L. G. Scantlebury Smead,[63] A. Scarabotto,[13] S. Schael,[14] S. Scherl,[60] M. Schiller,[59] H. Schindler,[48] M. Schmelling,[16] B. Schmidt,[48] S. Schmitt,[14] O. Schneider,[49] A. Schopper,[48] M. Schubiger,[32] S. Schulte,[49] M. H. Schune,[11] R. Schwemmer,[48] B. Sciascia,[23,48] S. Sellam,[46] A. Semennikov,[41] M. Senghi Soares,[33] A. Sergi,[24,c] N. Serra,[50] L. Sestini,[28] A. Seuthe,[15] Y. Shang,[5] D. M. Shangase,[87] M. Shapkin,[44] I. Shchemerov,[83] L. Shchutska,[49] T. Shears,[60] L. Shekhtman,[43,k] Z. Shen,[5] S. Sheng,[4] V. Shevchenko,[81] E. B. Shields,[26,f] Y. Shimizu,[11] E. Shmanin,[83] J. D. Shupperd,[68] B. G. Siddi,[21] R. Silva Coutinho,[50] G. Simi,[28] S. Simone,[19,i] N. Skidmore,[62] T. Skwarnicki,[68] M. W. Slater,[53] I. Slazyk,[21,e] J. C. Smallwood,[63] J. G. Smeaton,[55] A. Smetkina,[41] E. Smith,[50] M. Smith,[61] A. Snoch,[32] L. Soares Lavra,[9] M. D. Sokoloff,[65] F. J. P. Soler,[59] A. Solovev,[38] I. Solovyev,[38] F. L. Souza De Almeida,[2] B. Souza De Paula,[2] B. Spaan,[15] E. Spadaro Norella,[25,q] P. Spradlin,[59] F. Stagni,[48] M. Stahl,[65] S. Stahl,[48] S. Stanislaus,[63] O. Steinkamp,[50,83] O. Stenyakin,[44] H. Stevens,[15] S. Stone,[68,48] D. Strekalina,[83] F. Suljik,[63] J. Sun,[27] L. Sun,[73] Y. Sun,[66] P. Svihra,[62] P. N. Swallow,[53] K. Swientek,[34] A. Szabelski,[36] T. Szumlak,[34] M. Szymanski,[48] S. Taneja,[62] A. R. Tanner,[54] M. D. Tat,[63] A. Terentev,[83] F. Teubert,[48] E. Thomas,[48] D. J. D. Thompson,[53] K. A. Thomson,[60] H. Tilquin,[61] V. Tisserand,[9] S. T'Jampens,[8] M. Tobin,[4] L. Tomassetti,[21,e] X. Tong,[5] D. Torres Machado,[1] D. Y. Tou,[13] E. Trifonova,[83] S. M. Trilov,[54] C. Trippl,[49] G. Tuci,[6] A. Tully,[49] N. Tuning,[32,48] A. Ukleja,[36] D. J. Unverzagt,[17] E. Ursov,[83] A. Usachov,[32] A. Ustyuzhanin,[42,82] U. Uwer,[17] A. Vagner,[84] V. Vagnoni,[20] A. Valassi,[48] G. Valenti,[20] N. Valls Canudas,[85] M. van Beuzekom,[32] M. Van Dijk,[49] H. Van Hecke,[67] E. van Herwijnen,[83] M. van Veghel,[79] R. Vazquez Gomez,[45] P. Vazquez Regueiro,[46] C. Vázquez Sierra,[48] S. Vecchi,[21] J. J. Velthuis,[54] M. Veltri,[22,w] A. Venkateswaran,[68] M. Veronesi,[32] M. Vesterinen,[56] D. Vieira,[65] M. Vieites Diaz,[49] H. Viemann,[76] X. Vilasis-Cardona,[85] E. Vilella Figueras,[60] A. Villa,[20] P. Vincent,[13] F. C. Volle,[11] D. Vom Bruch,[10] A. Vorobyev,[38] V. Vorobyev,[43,k] N. Voropaev,[38] K. Vos,[80] R. Waldi,[17] J. Walsh,[29] C. Wang,[17] J. Wang,[5] J. Wang,[4] J. Wang,[3] J. Wang,[73] M. Wang,[3] R. Wang,[54] Y. Wang,[7] Z. Wang,[50] Z. Wang,[3] Z. Wang,[6] J. A. Ward,[56,69] N. K. Watson,[53] S. G. Weber,[13] D. Websdale,[61] C. Weisser,[64] B. D. C. Westhenry,[54] D. J. White,[62] M. Whitehead,[54] A. R. Wiederhold,[56] D. Wiedner,[15] G. Wilkinson,[63] M. Wilkinson,[68] I. Williams,[55] M. Williams,[64] M. R. J. Williams,[58] F. F. Wilson,[57] W. Wislicki,[36] M. Witek,[35] L. Witola,[17] G. Wormser,[11] S. A. Wotton,[55] H. Wu,[68] K. Wyllie,[48] Z. Xiang,[6] D. Xiao,[7] Y. Xie,[7] A. Xu,[5] J. Xu,[6] L. Xu,[3] M. Xu,[7] Q. Xu,[6] Z. Xu,[9] Z. Xu,[6] D. Yang,[3] S. Yang,[6] Y. Yang,[6] Z. Yang,[5] Z. Yang,[66] Y. Yao,[68] L. E. Yeomans,[60] H. Yin,[7] J. Yu,[71] X. Yuan,[68] O. Yushchenko,[44] E. Zaffaroni,[49] M. Zavertyaev,[16,t] M. Zdybal,[35] O. Zenaiev,[48] M. Zeng,[3] D. Zhang,[7] L. Zhang,[3] S. Zhang,[71] S. Zhang,[5] Y. Zhang,[5] Y. Zhang,[63] A. Zharkova,[83] A. Zhelezov,[17] Y. Zheng,[6] T. Zhou,[5] X. Zhou,[6] Y. Zhou,[6] V. Zhovkovska,[11] X. Zhu,[3] X. Zhu,[7] Z. Zhu,[6] V. Zhukov,[14,40] J. B. Zonneveld,[58] Q. Zou,[4] S. Zucchelli,[20,g] D. Zuliani,[28] and G. Zunica[62]

(LHCb Collaboration)

[1]*Centro Brasileiro de Pesquisas Físicas (CBPF), Rio de Janeiro, Brazil*
[2]*Universidade Federal do Rio de Janeiro (UFRJ), Rio de Janeiro, Brazil*
[3]*Center for High Energy Physics, Tsinghua University, Beijing, China*
[4]*Institute Of High Energy Physics (IHEP), Beijing, China*
[5]*School of Physics State Key Laboratory of Nuclear Physics and Technology, Peking University, Beijing, China*
[6]*University of Chinese Academy of Sciences, Beijing, China*
[7]*Institute of Particle Physics, Central China Normal University, Wuhan, Hubei, China*
[8]*Univ. Savoie Mont Blanc, CNRS, IN2P3-LAPP, Annecy, France*
[9]*Université Clermont Auvergne, CNRS/IN2P3, LPC, Clermont-Ferrand, France*
[10]*Aix Marseille Univ, CNRS/IN2P3, CPPM, Marseille, France*
[11]*Université Paris-Saclay, CNRS/IN2P3, IJCLab, Orsay, France*
[12]*Laboratoire Leprince-Ringuet, CNRS/IN2P3, Ecole Polytechnique, Institut Polytechnique de Paris, Palaiseau, France*
[13]*LPNHE, Sorbonne Université, Paris Diderot Sorbonne Paris Cité, CNRS/IN2P3, Paris, France*
[14]*I. Physikalisches Institut, RWTH Aachen University, Aachen, Germany*

[15]Fakultät Physik, Technische Universität Dortmund, Dortmund, Germany
[16]Max-Planck-Institut für Kernphysik (MPIK), Heidelberg, Germany
[17]Physikalisches Institut, Ruprecht-Karls-Universität Heidelberg, Heidelberg, Germany
[18]School of Physics, University College Dublin, Dublin, Ireland
[19]INFN Sezione di Bari, Bari, Italy
[20]INFN Sezione di Bologna, Bologna, Italy
[21]INFN Sezione di Ferrara, Ferrara, Italy
[22]INFN Sezione di Firenze, Firenze, Italy
[23]INFN Laboratori Nazionali di Frascati, Frascati, Italy
[24]INFN Sezione di Genova, Genova, Italy
[25]INFN Sezione di Milano, Milano, Italy
[26]INFN Sezione di Milano-Bicocca, Milano, Italy
[27]INFN Sezione di Cagliari, Monserrato, Italy
[28]Universita degli Studi di Padova, Universita e INFN, Padova, Padova, Italy
[29]INFN Sezione di Pisa, Pisa, Italy
[30]INFN Sezione di Roma La Sapienza, Roma, Italy
[31]INFN Sezione di Roma Tor Vergata, Roma, Italy
[32]Nikhef National Institute for Subatomic Physics, Amsterdam, Netherlands
[33]Nikhef National Institute for Subatomic Physics and VU University Amsterdam, Amsterdam, Netherlands
[34]AGH - University of Science and Technology, Faculty of Physics and Applied Computer Science, Kraków, Poland
[35]Henryk Niewodniczanski Institute of Nuclear Physics Polish Academy of Sciences, Kraków, Poland
[36]National Center for Nuclear Research (NCBJ), Warsaw, Poland
[37]Horia Hulubei National Institute of Physics and Nuclear Engineering, Bucharest-Magurele, Romania
[38]Petersburg Nuclear Physics Institute NRC Kurchatov Institute (PNPI NRC KI), Gatchina, Russia
[39]Institute for Nuclear Research of the Russian Academy of Sciences (INR RAS), Moscow, Russia
[40]Institute of Nuclear Physics, Moscow State University (SINP MSU), Moscow, Russia
[41]Institute of Theoretical and Experimental Physics NRC Kurchatov Institute (ITEP NRC KI), Moscow, Russia
[42]Yandex School of Data Analysis, Moscow, Russia
[43]Budker Institute of Nuclear Physics (SB RAS), Novosibirsk, Russia
[44]Institute for High Energy Physics NRC Kurchatov Institute (IHEP NRC KI), Protvino, Russia, Protvino, Russia
[45]ICCUB, Universitat de Barcelona, Barcelona, Spain
[46]Instituto Galego de Física de Altas Enerxías (IGFAE), Universidade de Santiago de Compostela, Santiago de Compostela, Spain
[47]Instituto de Fisica Corpuscular, Centro Mixto Universidad de Valencia - CSIC, Valencia, Spain
[48]European Organization for Nuclear Research (CERN), Geneva, Switzerland
[49]Institute of Physics, Ecole Polytechnique Fédérale de Lausanne (EPFL), Lausanne, Switzerland
[50]Physik-Institut, Universität Zürich, Zürich, Switzerland
[51]NSC Kharkiv Institute of Physics and Technology (NSC KIPT), Kharkiv, Ukraine
[52]Institute for Nuclear Research of the National Academy of Sciences (KINR), Kyiv, Ukraine
[53]University of Birmingham, Birmingham, United Kingdom
[54]H.H. Wills Physics Laboratory, University of Bristol, Bristol, United Kingdom
[55]Cavendish Laboratory, University of Cambridge, Cambridge, United Kingdom
[56]Department of Physics, University of Warwick, Coventry, United Kingdom
[57]STFC Rutherford Appleton Laboratory, Didcot, United Kingdom
[58]School of Physics and Astronomy, University of Edinburgh, Edinburgh, United Kingdom
[59]School of Physics and Astronomy, University of Glasgow, Glasgow, United Kingdom
[60]Oliver Lodge Laboratory, University of Liverpool, Liverpool, United Kingdom
[61]Imperial College London, London, United Kingdom
[62]Department of Physics and Astronomy, University of Manchester, Manchester, United Kingdom
[63]Department of Physics, University of Oxford, Oxford, United Kingdom
[64]Massachusetts Institute of Technology, Cambridge, Massachusetts, USA
[65]University of Cincinnati, Cincinnati, Ohio, USA
[66]University of Maryland, College Park, Maryland, USA
[67]Los Alamos National Laboratory (LANL), Los Alamos, USA
[68]Syracuse University, Syracuse, New York, USA
[69]School of Physics and Astronomy, Monash University, Melbourne, Australia
(associated with Department of Physics, University of Warwick, Coventry, United Kingdom)
[70]Pontifícia Universidade Católica do Rio de Janeiro (PUC-Rio), Rio de Janeiro, Brazil
(associated with Universidade Federal do Rio de Janeiro (UFRJ), Rio de Janeiro, Brazil)
[71]Physics and Micro Electronic College, Hunan University, Changsha City, China
(associated with Institute of Particle Physics, Central China Normal University, Wuhan, Hubei, China)

[72]Guangdong Provincial Key Laboratory of Nuclear Science, Guangdong-Hong Kong Joint Laboratory of Quantum Matter, Institute of Quantum Matter, South China Normal University, Guangzhou, China
(associated with Center for High Energy Physics, Tsinghua University, Beijing, China)
[73]School of Physics and Technology, Wuhan University, Wuhan, China
(associated with Center for High Energy Physics, Tsinghua University, Beijing, China)
[74]Departamento de Fisica, Universidad Nacional de Colombia, Bogota, Colombia
(associated with LPNHE, Sorbonne Université, Paris Diderot Sorbonne Paris Cité, CNRS/IN2P3, Paris, France)
[75]Universität Bonn—Helmholtz-Institut für Strahlen und Kernphysik, Bonn, Germany
(associated with Physikalisches Institut, Ruprecht-Karls-Universität Heidelberg, Heidelberg, Germany)
[76]Institut für Physik, Universität Rostock, Rostock, Germany
(associated with Physikalisches Institut, Ruprecht-Karls-Universität Heidelberg, Heidelberg, Germany)
[77]Eotvos Lorand University, Budapest, Hungary
(associated with European Organization for Nuclear Research (CERN), Geneva, Switzerland)
[78]INFN Sezione di Perugia, Perugia, Italy
(associated with INFN Sezione di Ferrara, Ferrara, Italy)
[79]Van Swinderen Institute, University of Groningen, Groningen, Netherlands
(associated with Nikhef National Institute for Subatomic Physics, Amsterdam, Netherlands)
[80]Universiteit Maastricht, Maastricht, Netherlands
(associated with Nikhef National Institute for Subatomic Physics, Amsterdam, Netherlands)
[81]National Research Centre Kurchatov Institute, Moscow, Russia
(associated with Institute of Theoretical and Experimental Physics NRC Kurchatov Institute (ITEP NRC KI), Moscow, Russia)
[82]National Research University Higher School of Economics, Moscow, Russia
(associated with Yandex School of Data Analysis, Moscow, Russia)
[83]National University of Science and Technology "MISIS", Moscow, Russia
(associated with Institute of Theoretical and Experimental Physics NRC Kurchatov Institute (ITEP NRC KI), Moscow, Russia)
[84]National Research Tomsk Polytechnic University, Tomsk, Russia
(associated with Institute of Theoretical and Experimental Physics NRC Kurchatov Institute (ITEP NRC KI), Moscow, Russia)
[85]DS4DS, La Salle, Universitat Ramon Llull, Barcelona, Spain
(associated with ICCUB, Universitat de Barcelona, Barcelona, Spain)
[86]Department of Physics and Astronomy, Uppsala University, Uppsala, Sweden
(associated with School of Physics and Astronomy, University of Glasgow, Glasgow, United Kingdom)
[87]University of Michigan, Ann Arbor, USA
(associated with Syracuse University, Syracuse, NY, USA)

[a]Deceased.
[b]Also at Università di Firenze, Firenze, Italy.
[c]Also at Università di Genova, Genova, Italy.
[d]Also at Università di Modena e Reggio Emilia, Modena, Italy.
[e]Also at Università di Ferrara, Ferrara, Italy.
[f]Also at Università di Milano Bicocca, Milano, Italy.
[g]Also at Università di Bologna, Bologna, Italy.
[h]Also at Università di Roma Tor Vergata, Roma, Italy.
[i]Also at Università di Bari, Bari, Italy.
[j]Also at Università di Cagliari, Cagliari, Italy.
[k]Also at Novosibirsk State University, Novosibirsk, Russia.
[l]Also at Universidade Federal do Triângulo Mineiro (UFTM), Uberaba-MG, Brazil.
[m]Also at Hangzhou Institute for Advanced Study, UCAS, Hangzhou, China.
[n]Also at Università di Siena, Siena, Italy.
[o]Also at Università di Padova, Padova, Italy.
[p]Also at Scuola Normale Superiore, Pisa, Italy.
[q]Also at Università degli Studi di Milano, Milano, Italy.
[r]Also at MSU—Iligan Institute of Technology (MSU-IIT), Iligan, Philippines.
[s]Also at Excellence Cluster ORIGINS, Munich, Germany.
[t]Also at P.N. Lebedev Physical Institute, Russian Academy of Science (LPI RAS), Moscow, Russia.
[u]Also at Università di Pisa, Pisa, Italy.
[v]Also at Università della Basilicata, Potenza, Italy.
[w]Also at Università di Urbino, Urbino, Italy.